ENHANCEMENT OF SYNERGISTIC EFFECT PHOTOCATALYTIC/PERSULFATE ACTIVATION FOR DEGRADATION OF AGRO PESTICIDES RESIDUES BY TERNARY NANOCOMPOSITE ZnO/TiO_2/MgO

NÂNG CAO HIỆU ỨNG TƯƠNG HỖ HOẠT HÓA QUANG XÚC TÁC/PERSULFATE ĐỂ PHÂN HỦY DƯ LƯỢNG THUỐC BẢO VỆ THỰC VẬT BẰNG NANOCOMPOZIT ĐA OXIT BẬC BA ZnO/TiO_2/MgO

Nguyen Dinh Tuyen[1,*], Nguyen Thi Thu An[2], Nguyen Quyet Tien[1], Nguyen Quang An[1], Nguyen Ngoc Truong[3], Nguyen Thi Thuc Anh[3], Nguyen Huy Cuong[3], Le Thi Trang[3], Nguyen Thi Mai[4]

DOI: https://doi.org/10.57001/huih5804.2023.261

ABSTRACT

In this study we present a method to synthesize new heterogenous photocatalytic materials based on ternary nanocomposite ZnO/MgO/TiO_2 to activate persulphate ($K_2S_2O_8$) for degradation of methylen blue dye (MB) and pesticide acetamiprid that used in aquaculture and agricultural cultivation under simulated sunlight. Photocatalytic composite samples with nano nanostructures were synthesized by hydrothermal method in an alkaline medium and characterized by X-ray diffraction (XRD), Electron absorption spectrum (UV-Vis), N_2 absorption/desorpions (BET), High-resolution Transmission Electron Microscopy (TEM), Fourier Transform Infrared Spectroscopy (FTIR), Energy Dispersive X-ray Spectroscopy (EDX), Zeta potential measurement, Differential thermogravimetric method (TG-DTA), Decomposition activity of Methylen Blue and pesticides Acetamiprid over multi-oxides composite under simulated sunlight when used separatetly and in combination with persulfate ($K_2S_2O_8$), with photocatalyst dose of 100 mg/L, irradaried intensity of 800μW/cm^2, has been investigated over reaction time. The synergistic photocatalytic activation properties of persulfate by ZnO/TiO_2/MgO material to decompose the pesticides and dye in aqueous solution also were investigated. The results showed that the composite photocatalytic material has shown excellent synergistic properties of the heterogeneous photocatalyst ZnO/TiO_2/MgO-persulfate system in enhancing the decomposition of Methylen Blue and Acetamiprid residues in the water solution. The research results also show that the photocatalytic material ZnO/TiO_2/MgO- persulfate system has potential for practical application to control diseases and treat contaminated environments in aquaculture and organic agricultural crop cultivation.

Keywords: *Pesticides, heterogeneous photocatalysis, activated persulfate, synergistic effect, multi oxides, ZnO/MgO/TiO_2*

TÓM TẮT

Trong nghiên cứu này, chúng tôi trình bày phương pháp tổng hợp vật liệu quang xúc tác dị thể mới trên cơ sở nanocompozit ba phân tử ZnO/MgO/TiO_2 để hoạt hóa Persulphate ($K_2S_2O_8$) nhằm phân hủy thuốc nhuộm xanh methylen (MB) và thuốc trừ sâu acetamiprid sử dụng trong nuôi trồng thủy sản và trồng trọt nông nghiệp dưới ánh sáng mặt trời mô phỏng. Các mẫu tổ hợp quang xúc tác có cấu trúc nano được tổng hợp bằng phương pháp thủy nhiệt trong môi trường kiềm và được đặc trưng bởi các phương pháp nhiễu xạ Rơn gen XRD, Phổ hấp thụ điện tử (UV-Vis), Hấp thụ/giải hấp nito (BET), Hiển vi điện tử truyền qua phân giải cao (TEM), Quang phổ hồng ngoại biến đổi Fourier (FTIR), Quang phổ tia X tán sắc năng lượng (EDX) , Đo điện thế Zeta, Phương pháp đo nhiệt vi phân sai (TG-DTA)... Hoạt tính phân hủy của Methylen Blue và thuốc trừ sâu Acetamiprid trên tổ hợp đa oxit dưới ánh sáng mặt trời mô phỏng khi sử dụng riêng lẻ và kết hợp với Persulfate ($K_2S_2O_8$), với liều lượng xúc tác quang 100 mg/L, cường độ chiếu xạ 800μW/cm^2, đã được nghiên cứu. Tính chất hoạt hóa quang xúc tác tổng hợp của Persulfate bằng vật liệu ZnO/TiO_2/MgO để phân hủy thuốc trừ sâu và thuốc nhuộm trong dung dịch nước cũng đã được nghiên cứu. Kết quả cho thấy vật liệu quang xúc tác composite đã thể hiện tính chất hiệp đồng tuyệt vời của hệ xúc tác quang dị thể ZnO/TiO_2/MgO-persulfate trong việc tăng cường khả năng phân hủy dư lượng Methylen Blue và Acetamiprid trong dung dịch nước. Kết quả nghiên cứu cũng cho thấy hệ vật liệu quang xúc tác ZnO/TiO_2/MgO-persulfate có tiềm năng ứng dụng thực tế để kiểm soát dịch bệnh và xử lý môi trường ô nhiễm trong nuôi trồng thủy sản và canh tác cây nông nghiệp hữu cơ.

Từ khóa: *Thuốc trừ sâu, quang xúc tác dị thể, persulfate hoạt hóa, tác dụng hiệp đồng, đa oxit, ZnO/MgO/TiO_2.*

[1]Institute of Chemistry, Vietnam Academy of Science and Technology, Viet Nam
[2]Institute of Biotechnology, Vietnam Academy of Science and Technology, Viet Nam
[3]Institute of Applied Geology and Minerals Research,Vietnam
[4]Center for High Technology Development, Vietnam Academy of Science and Technology, Viet Nam
[*]Email: tuyenndvast@gmail.com
Received: 25/10/2023
Revised: 19/12/2023
Accepted: 25/12/2023

1. INTRODUCTION

The abuse of pesticides leads to toxic residues in agricultural products (active ingredients imidacloprid, acetamiprid, fipronil, abamectin, etc) often exceeding the allowable threshold, reducing value of the product, directly affecting the health of workers and consumers, causing environmental pollution and imbalance in the agricultural ecosystem [1, 5]. Finding solutions to reduce pollutants, improve the quality of agricultural products, and limit negative impacts caused by using pesticides on the environment is very urgent. Currently, new photocatalytic materials based on multi-oxide composites including single oxides or modified multi oxides of transition metals Ti, Zn, Cu, Ag, Bi, V, Mn, Mo, Se, Si, Mg… [6-9] can replace pesticides in treating some pathogenic microorganisms [19,20]. Especially when modified multi oxides were intergrated with persulfate, they will create synergistic effects, improving bactericidal effectiveness and gradually decomposing and mineralization toxic residues through the radical mechanism with reactive oxygen species (ROS) [6-10].

The photocatalytic process belongs to the category of Advanced oxidation processes (AOPs), on the one hand generate reactive oxygen species - ROS such as free radicals (•OH), ($SO4^{\bullet-}$), ($O2^{\bullet-}$) on the particles surface that strongly oxidize destroy of pathogens and on the other hand also degradates and mineralize of pesticides residues. AOPs technologies with uses friendly multi-oxide nanomaterials composites in oder to reduce the use and or replace amount of pesticides and antibiotics in the aquaculture, and agricultural farming are being intensively researched [5, 6, 13]. Most AOPs are based on the hydroxyl radical (•OH), superoxide radical ($O2^{\bullet-}$) generation, but in recent years methods based on the sulfate radical ion ($SO4^{\bullet-}$) when using photocatlytic actived-persulfate have gained popularity (In situ chemical oxidation (ISCO) process) [6-10].

Figure 1. Mechanizm of photocatalytic degradation of pesticides and microorganisms on the multi oxides surface [12]

As known persulfate (peroxydisulfate (PDS, $S_2O_8^{2-}$) or peroxymonosulfate (PMS, HSO_5^-) itself has no oxidation activety and they need to activate by many ways to produce sulfate radicals in reaction system [6-10]. The activation of persulfate by transition metal oxides as heterogeneous photocatalytic systems is more cost-effective than thermal [12-20], ultraviolet photochemical [14,15], ultrasonical, electrochemical, base; metals and metal oxides, organic compunds, non-metal composite biochar, activated carbon, graphene, cacbon nitrite g-C_3N_4, etc. Although various photocatalysts activators based on transition metal oxides have been fabricated to activate PMS such as binary oxides, ternary oxides, quaternary oxides ($CuCo_2O_4$, Fe_2O_3/SiO_2, Zn-MgO, CuO-ZnO, TiO_2-MgO, Ag_2O- Fe_2O_3-ZnO-TiO_2, etc). The use of ternary oxides based on ZnO, MgO and TiO_2 gained advantages: reduce the speed of photogenerated carrier recombination observably increase the degradation efficiency of the contaminants; reduce the metal ion leaching from tenary oxides composite, which will lead to reduce secondary environmental pollution; and starting material for synthesis of materials have a low cost [12, 13, 19, 20].

When persulfates (peroxydisulfate PS, $S_2O_8^{2-}$) or peroxymonosulfate (PMS, HSO_5^-) is added to the reaction system with multi oxides as photocatalytic activator (Fig. 2b), more highly reactive free radicals of $SO4^{\bullet-}$/•OH/$O_2^{\bullet-}$ are produced, and the separation efficiency of the photogenerated carriers is enhanced compared to that without persulfates [5, 12];

$$\text{Photocatalyst} + h\sqrt{} \rightarrow e^{CB-} + h^{VB+}$$

$$\text{PDS/PMS} + \text{photocatalyst} + h\sqrt{} \rightarrow (SO_4^{\bullet-}) + (\bullet OH) + (O_2^{\bullet-})$$

$$S_2O_8^{2-} + e^- \rightarrow SO_4^{\bullet-} + SO_4^{2-}$$

$$SO_4^{\bullet-} + H_2O \rightarrow SO_4^{2-} + {}^{\bullet}OH + H$$

$$HSO_5^- \rightarrow SO_4^{\bullet-} + \bullet OH$$

$$h^{VB+} + H_2O \rightarrow \bullet OH + H^+$$

$$SO_4^{\bullet-}/\bullet OH/\ O_2^{\bullet-} + \text{pesticides} + \text{live microorganisms} \rightarrow \text{degradation products}$$

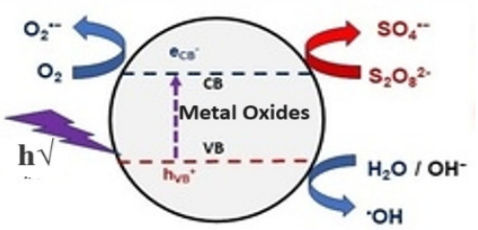

Figure 2. Mechanism of photocatalytic activation of persulfate by multi oxides materials, under visible light irradiation [6]

. In this study, we present results of preparation of new composite photocatalysts based on ternary oxides composite ZnO/MgO/TiO_2 high synergistic effects to activate persulfate (PS) under sunlight, focus on the explore practical application potential of these photocatalyst materials to replace or reduce toxic residues of some pesticides that are being widely used in agriculture on post-harvest agricultural products.

2. EXPERIMENTAL

2.1. Chemicals and materials

Titanium dioxide anatas KA100 (TiO_2, Korea, 98%), Sodium hydroxide NaOH, (China, 98%), Magnesium Oxide MgO (95%, China), Zinc Oxide ZnO (95%, Malaysia), Acetamiprid $C_{10}H_{11}ClN_4$ (Aldrich Sigma, 99.5%), peroxydisulfate $K_2S_2O_8$ (98%, Japan).

2.2. Synthesis of materials

Preparation of multi-metal oxide composite $ZnO/MgO/TiO_2$ with slight modified [13]. Add 730 ml of NaOH solution (3M) and 20 grams of $ZnO/MgO/TiO_2$ prepared mixture with the weight ratio $ZnO:MgO:TiO_2$ of 4:2:1 in the refluxed glass vase 1000 ml. The mixture was heated and stirred at 120°C for 24 hours. Filter, wash and neutralize the resulting solid with distilled water several times to pH = 7.5; Dry the obtained solid at 180°C for 8 hours then calcine at 450°C for 5 hours. The material sample named HHM.

2.3. Characterization of the material

The material was characterized by Fourier transform infrared spectroscopy (FTIR) on an Impact-410 machine (Germany), Differential thermogravimetric method (TG-DTA), Energy Dispersive X-ray Spectroscopy (EDX) on a Jeol-JMS 6490 equipments at the Institute of Tropical Technology, Vietnam Academy of Science and Technology (VAST). X-ray diffraction (XRD) of samples were analyzed on a D8 Advance diffraction merrter; N_2 absorption/desorpions (BET) measured on a Tristar-3030 instrument (GA USA); High-resolution transmission electron microscopy (TEM) using a H-7500 (HITACHI, Japan) at the National Institute of Hygiene and Epidemiology; UV-Vis electron absorption spectrum of the sample was measured on a GBC Instrument-2885 in the step region Waves from 200 - 800nm (Department of Physics, Hanoi National University). Zeta potential measurement method wereused at the Institute of Materials Science (VAST). The sunlight intensity was measured by a solar power meter (SM206).

2.4. Evaluation of photodegradation efficences of pesticides Acetamiprid and methylene Bue dye in aqueous solutions

Add 10mg of HHM material into a glass beaker (500ml) containing 100ml of Acetamiprid solution (10ppm)/Methylen Blue (30ppm), stir at 500rpm in the dark to achieve adsorption equilibrium. Take liquid samples 4.0 ml at reaction times of 30 minutes, 60 minutes, 120 minutes and 180 minutes; centrifugal; filtere through a membrane filter (4.5 micrometers) to separate solid particles and then analyzed liquid samples on a UV-Vis absorption spectra equipment.

The photocatalytic experiment was performed similarly as above, but the beakers were illuminated by simulated sunlight lamp (Kosmetic Brauner Typ-826). Methylen Blue and Acetamipride concentration was determined by absorbance at 664nm and 246nm wavelength and calculated according to the standard curve method .

The removal efficiency of MB and pesticide was calculated from the following equation:

$$\text{Removal efficiency (\%)} = ((C_0 - C_e)/C_0) \times 100 \quad (1)$$

C_0 is the initial absorbance and C_e is absorbance after treatment.

The photocatalytic degradation activity of materials is calculated according to the formula:

$$q = \frac{(C_o - C_t)V}{m}, \text{(mg/g)} \quad (2)$$

Where C_o is the initial concentration of Acetamiprid and Methylen Blue, mg/l; C_t is the concentration of Acetamiprid and Methylen Blue at treatment time t, mg/l; V is the volume of Acetamiprid and Methylen Blue aqueous solution, l; m is mass weight of the material (g).

3. RESULTS AND DISCUSSION

3.1. XRD pattern and FTIR spectra

XRD spectrum (Figure 3) shows that the characteristic diffraction peaks of ZnO structures were observed at around 2θ = 31.5° - 34.3° - 36.2° - 46.5° and 48.2°. Diffractions peaks at 2θ = 36.0° - 44.2° and 62.0° were detected and attributed to MgO structure, and TiO_2 anatase phase of TiO_2 corresponding to peaks at at angle 2θ = 25.2° - 31.5° - 48.2°. Nevertheless, the presence of each oxides ZnO, TiO_2 and MgO did not promote significant changes in the material matrix. The displacement of the reflections was due to a slight modification in the crystals phase, promoting the incorporation of the dopant materials into the composition network [13,19,20]

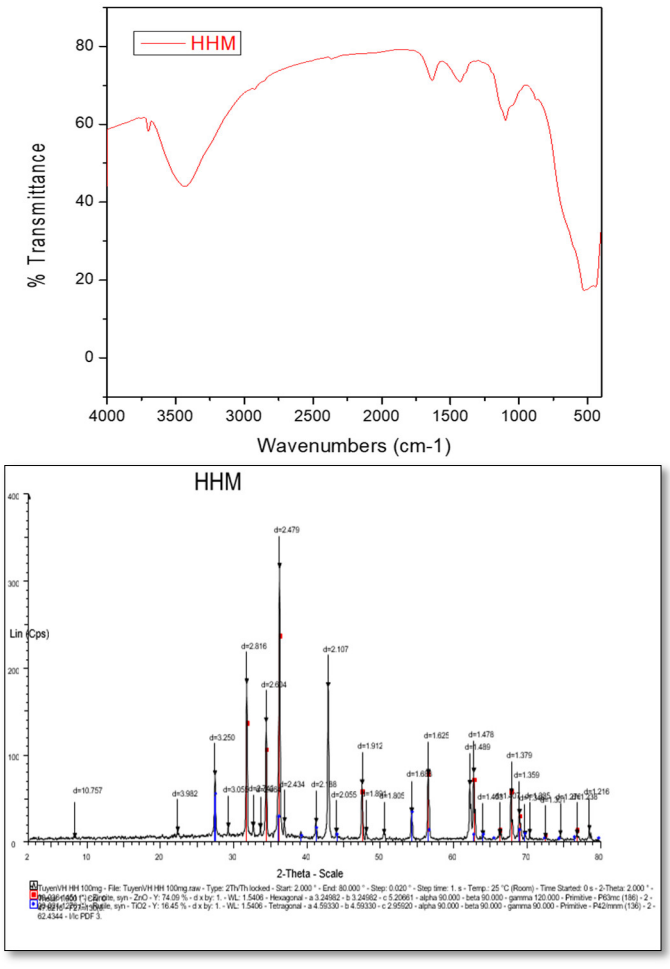

Figure 3. XRD pattern and FTIR spectra of ZnO /MgO /TiO_2

Figure 3 shows the FTIR spectra of multi oxides composite recorded in the range from 4000 to 400cm^{-1}, bands at 667, 654, 604 and 543cm^{-1} were observed and the fuctuations in these regions are typical of the anatase TiO_2 structure [12,13] and is related to the elongation mode of Ti–OH, Ti–O and O–Ti–O bonds. Additionally, a band of about 545cm^{-1} was detected in the samples due to the presence of Zn–O bonds. Furthermore, a band at 667cm^{-1} was detected, confirmed the presence of MgO vibrations. The absorption band is about 1600cm^{-1} attributed to O–H fluctuations related to physically adsorbed water in the samples [12-14].

3.2. TEM

From Figure 4, the TEM image of the material shows that HHM multi-metal oxide nanomaterial has a composite nano structure, the particles are evenly distributed, the particle size is uniform around 100nm.

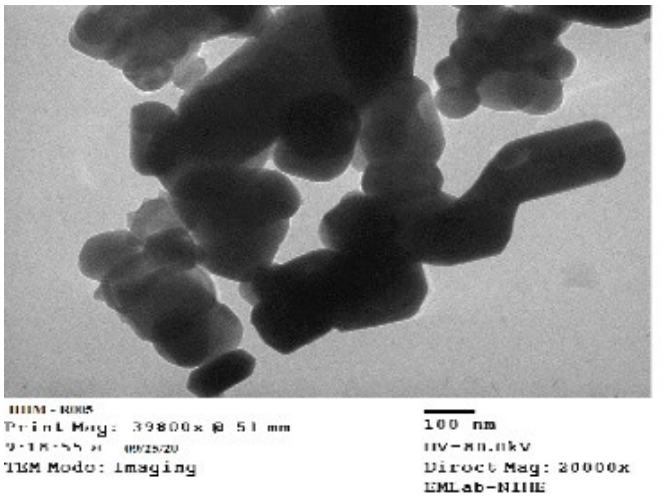

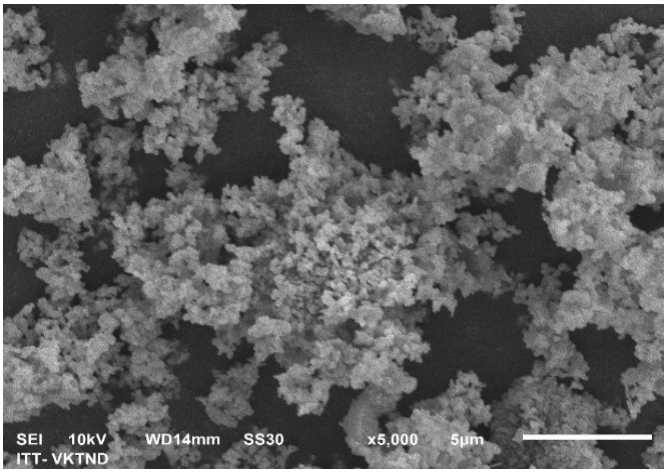

Figure 4. TEM image of HHM samples

3.3. BET

Nitrogen adsorption-desorption isotherms (BET) results show that the specific surface of the HHM composite material is 8.28m^2/g. However, the synthesized material has an average capillary zone (meso/macro pores) due to the formation of voids between nano particles with an average pore diameter of 19.22nm and a pore volume of 0.046cm^3/g.

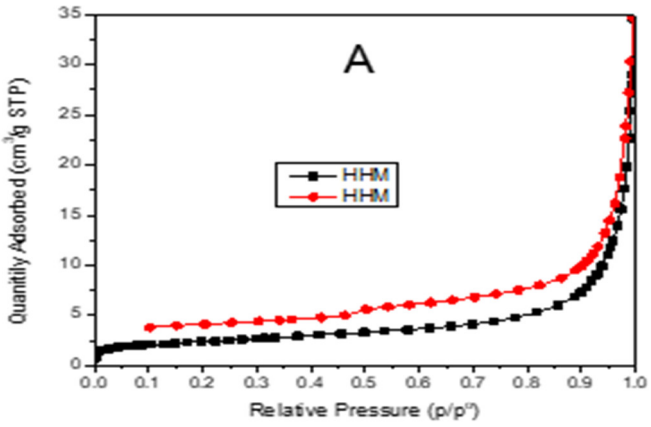

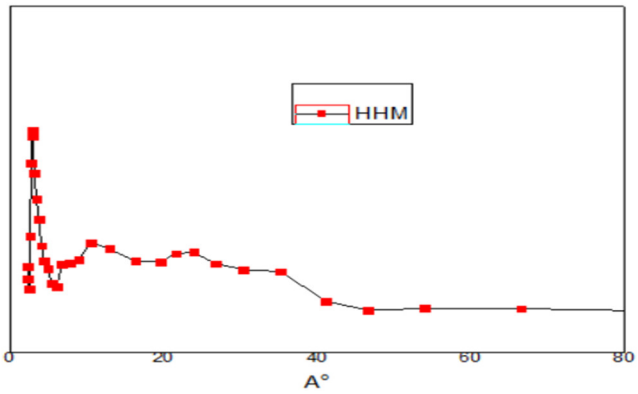

Figure 5. Nitrogen adsorption–desorption isotherms and pore size distribution of HHM sample

3.4. EDX spectra

From the elemental composition by energy dispersive spectroscopy (EDS) results (Fig. 6, Table 1), we could see that the atom ratio of each metals in synthezed composite Zn: Mg: Ti ~ 1,8 :1:1,2 and so synthesized material through the hydrothermal process in strong akali medium was corresponds to the initial mixture composition ratio, proving the ZnO/MgO/TiO_2 particles were formed and distributed evenly [12, 14, 20]. That is also clearly seen on the IR spectrum and TEM images of the HHM samples (Fig. 4).

Table 1. Elements Component of HHM

Element	Weight, %	Atomic, %
O	30.55	55.40
Mg	7.61	9.08
Ti	18.07	10.94
Zn	39.02	17.32
Al	0.56	0.60
Na	2.41	3.04
C	1.37	3.32
Ca	0.17	0.12
Si	0.10	0.10
Fe	0.15	0.08
Total	100.00	100.00

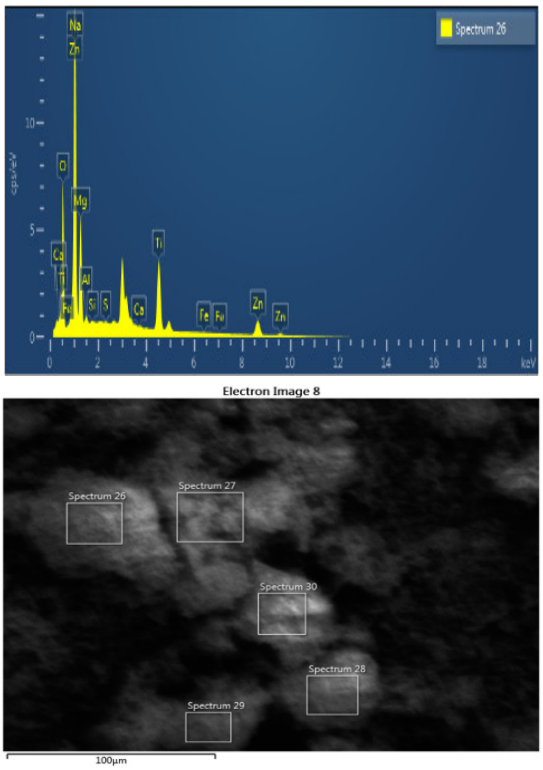

Figure 6. EDX spetrum of HHM samples

3.5. UV-Vis spectra

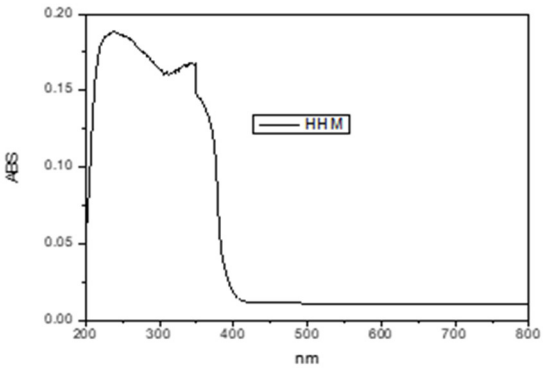

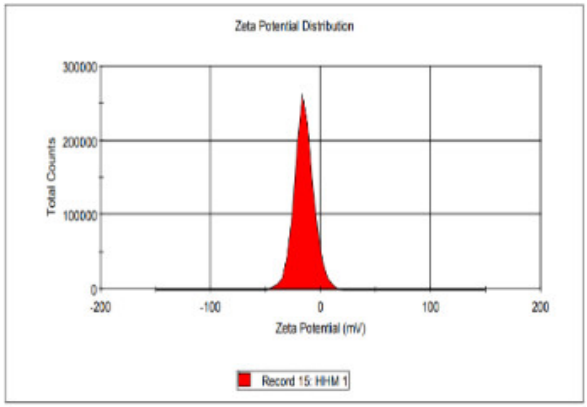

Figure 7. UV-Vis spectra of HHM samples and Zeta potential of HHM sample

The UV-Vis spectra studies show that the photocatalysts HHM has strong absorption in the visible light region. From Fig. 6, it can be seen absorption peak that shifts toward the visible light region, meaning its ability absorb sunlight is significantly improved. The bandgap energies of the catalysts were estimated using the formula $E_b = h*C/\lambda > Eb = 1240/\lambda_g$ (critical wavelength); the band gap energy E_b (HHM) = 1, 98eV ; λ_g = 624nm respectively.

3.6. Zeta potential

From Figure 7, it can be seen that the HHM composite material sample has negative surface charge with Zeta potential = -15.2 (mV) (pH = 7.0). As is known, the separate oxide components ZnO and TiO_2 usually have positive Zeta potential at pH = 7.0, only MgO oxide has a negative charge, so when forming tenary composites, the Zeta potential charge will be negative it does means that there were chemical interractions between ZnO, MgO and TiO_2 nanoparticles [15, 20].

3.7. Thermal gravimetric analysis TGA

Thermogravimetric analysis results of the material sample (Figure 8) show weight loss due to decomposition of water and multi oxides structure in the temperature range of 100°C and above 600°C. The thermal stability of the composite HHM may be attributed to the presence of chemical interactions of each oxides in composite HHM when tenary composites was formed [15-20].

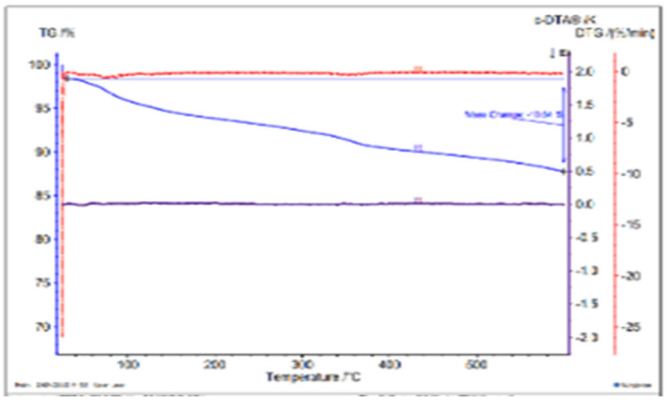

Figure 8. TGA diagram of HHM samples

3.8. Photocatalytic degradation MB over HHM and synergistic effects in photocatalytic activated persulfate system

With a very small amount of HHM material in the reaction solution (10mg of material in a volume of 100ml of 30ppm MB solution), the MB concentration in the dark is almost constant and the process occurring on the surface of the catalyst particles is only adsorption process (*curve* a). However, when there is illumination, the decrease in MB in the solution is (8%), proving that photocatalytic decomposition of MB on HHM material has occurred (*curve* c). In the presence of PS (500mg) without light, the conversion of MB almost did not occur (*curve* b), but when light was present, PS was activated by light energy to enhancing the production of hydroxyl, sulphate and superoxide radicals that oxidizes and decomposes MB, clearly reducing the MB concentration in solution and the conversion reaching 35% (*curve* d).

Especially when both HHM and PS photocatalytic materials are present simultaneously, both in the dark and when illuminated, the MB concentration drops sharply and reaches 81 % and 95% removal efficents, respectively (*curve* e, f). This proves that PS were activated by both of light and photocatalyst HHM arcording to the mechanism in Fig. 1, Fig. 2 and the synergistic effect has occurred in the HHM-PS-light heterojunction system.

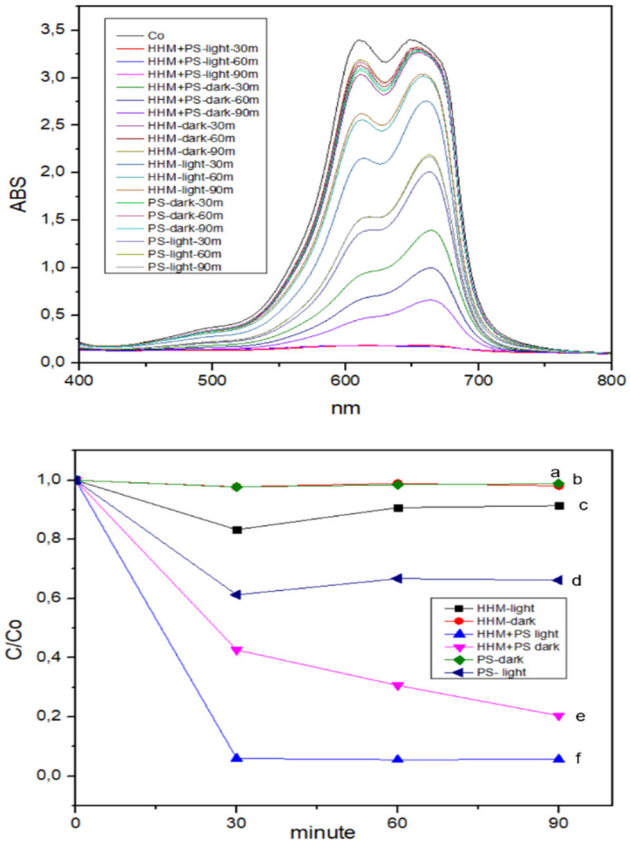

Figure 9. The UV-vis absorption spectra of MB during the photocatalytic degradation over tenary oxides HHM and Photocatalytic Degradation of MB in PS-HHM-system

Table 2. Degradation efficiency for MB, %

Materials and conditions	30 min	60 min	90 min
HHM (100ml MB 18ppm, *catalyst amount 10mg; in dark)* (b)	2.18	1.05	1.88
HHM (10mg) (100ml MB 18ppm, *catalyst amount 10mg; light intensity 800μW/cm²)* (c)	16.67	9.23	8.59
Persulfate $K_2S_2O_8$ (50mg), 100ml MB *18ppm*, in dark) (a)	2.26	1.50	1.14
Persulfate $K_2S_2O_8$ (50mg, 100ml MB 18ppm, *light intensity 800μW/cm²*) (d)	70.34	69.05	59.74
HHM (10mg) + persulfate $K_2S_2O_8$ (50mg), 100ml MB 18ppm, in dark) (e)	55.03	72.74	80.93
HHM (10mg) + persulfate $K_2S_2O_8$ (50mg); 100ml MB 18ppm, in dark) (f)	94.01	94.42	94.30

Table 3. Photocatalytic degradation activity of MB under various conditions, q, mg/g

Materials/conditions	C_t (30min), ppm	C_t (60min), ppm	C_t (90min) ppm	q_t (30min)	q_t (60min)	q_t (90min)
PS, dark (a)	17.89	18.03	18.10	1.38	0.91	0.69
HHM, dark (b)	17.91	18.11	17.96	1.33	0.64	1.15
HHM, light (c)	15.25	16.61	16.73	10.19	5.65	5.26
PS, light (d)	5.43	5.67	7.37	42.93	42.14	36.46
HHM+PS, dark (e)	8.23	4.99	3.49	33.58	44.39	49.39
HHM+PS, light (f)	1.10	1.02	1.04	57.37	57.62	57.55

C_t - Concentration of MB in aqueous solution, mg/L

q_t - amount of MB degradation per an amount of HHM materials, mg/g

3.9. Synergistic effects in photocatalytic activated persulfate degradation of Acetamiprid

Similar to the case of MB degradation above, the photocatalytic decomposition of the pesticide Acetamiprid aqueious solution also shows a synergistic effect in the HHM - PMS suspension system with a very small solid-liquid phase ratio in the mix solution.

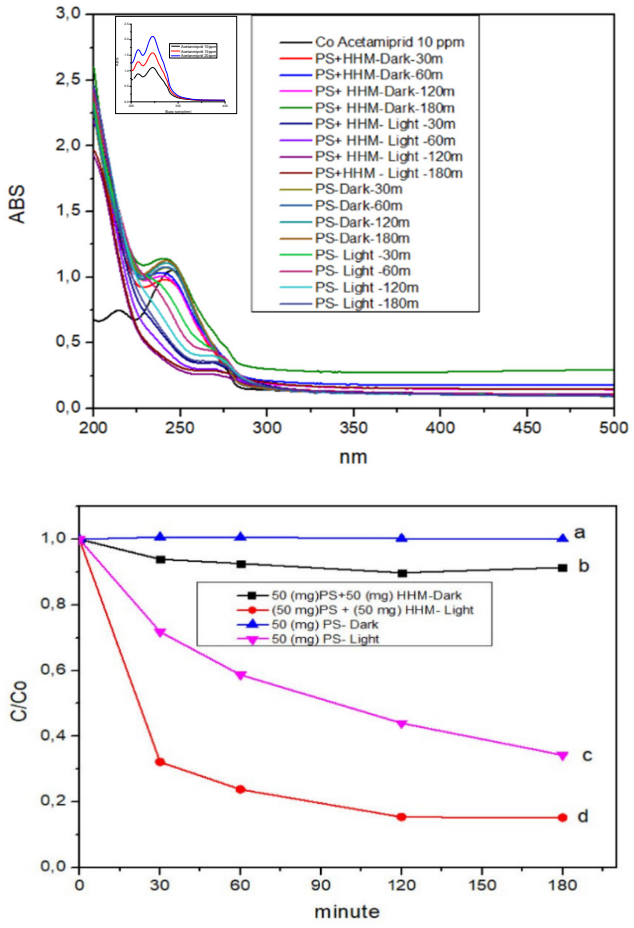

Figure 10. The UV-vis absorption spectra of Acetamiprid during the photocatalytic degradation over HHM and Photocatalytic Degradation of Acetamiprid in PS-HHM- heterogenous system

Table 4. Degradation efficiency of acetamiprid %

Reaction time	30 min	60 min	120 min	180 min
HHM (50mg) + PS (50mg), 100ml, light (d)	67.05	75.32	84.43	85.25
HHM (50mg) + PS (50mg), 100ml, dark (b)	5.10	8.05	12.25	13.85
PS (50mg), 100ml, dark (a)	0.25	0.45	0.45	0.50
PS (50mg), 100ml, light (c)	28.20	42.55	54.25	62.88

From the Fig. 10 and Table 4 it can be seen that PS ($K_2S_2O_8$) itself does not activate without at least one of the activating agents such as catalyst or light irradiation (*curve* a). If photocatalytic materials HHM and PS are present in solution, the activation of PS begein to started to create active radicals to oxidize and decompose organic matter Acetamiprid in the reaction solution (*curve* b). But PS itself was strongly activated by light irradiation to create active radicals to degradation of acetamiprid in solution (*curve* c). When photocatalytic materials HHM and PS are present in solution with illumination, acetamiprid concentration reduced sharply and reaches 85% of degradation efficiency within 180 minutes (*curve* d). This proves that PS was simultaneously activated by both the multi-oxide composite photocatalytic material and irradiated light. It can be explained that the synergistic effects in the HHM-PS heterogenous system - light were activated persulfate strongly to increase the density of radicals in the solution and the rate of decomposition of the pesticide acetamiprid [15, 16].

4. CONCLUSION

Ternary $ZnO/MgO/TiO_2$ multi-oxide composite photocatalytic material (HHM) with optimal composition ratio has been successfully synthesized. Research results show that photocatalytic materials are very effective in treating toxic pesticides residues in agricultural cultivation. The HHM/Acetamiprid/Persulfate ($K_2S_2O_8$)-integrated system and photocatalytic synergistic effects have been clearly demonstrated and that can be explained by the extreamly hightly generating rate of reactive free radicals of $SO4^{\bullet-}/\bullet OH/O_2^{\bullet-}$. This integrated system has a multi function that can destroy pathogen bacteria also decomposes pesticide residues, leading to the ability to use a pesticide product without residues under sunlight. The results of this research have opened up a new method applying the photocatalytic material ZnO/TiO_2/MgO-persulfate system to treat microorganism pathogens diseases applied in the aquatic farming and organic agricultural cultivation. Although there have been some practical application results for this type of materials. However, the phytoxicity to plants and aquatic life when using the -persulfate photocatalytic integrated system needs further research to clarify.

ACKNOWLEDGEMENT

The work is supported by the program for Senior Researchers of the Vietnam Academy of Science and Technology, project code NCVCC06.01/23-23

REFERENCES

[1]. Alia Servin, Wade Elmer, Arnab Mukherjee, Roberto De la Torre-Roche, Helmi Hamdi Jason C. White, Prem Bindraban, Christian Dimkpa, 2015. *A review of the use of engineered nanomaterials to suppress plant disease and enhance crop yield*. Journal of Nanoparticle Research, February.

[2]. Rope Yijian, Shen Canduo, Chen Changmin, 2018. *Advanced treatment method for pesticide residues on surfaces of fruits and vegetables*. Patent, CN104206937A

[3]. Joanne Gamage McEvoy, Zisheng Zhang, 2014. *Antimicrobial and photocatalytic disinfection mechanisms in silver-modified photocatalysts under dark and light conditions*. Journal of Photochemistry and Photobiology C: Photochemistry Reviews 19, 62–75

[4]. Vicente Rodríguez-Gonzáleza, Chiaki Terashimaa, Akira Fujishimaa, 2019. *Applications of photocatalytic titanium dioxide-based nanomaterialsin sustainable agriculture*, Journal of Photochemistry and Photobiology C: Photochemistry Reviews 40, 49-67.

[5]. Stewart B. Averett, Devron R. Averett, 2012. *Titanium dioxide photocatalytic compositions and uses thereof*. United States Patent, S8609121B2

[6]. Dongqi Tian, Hongyu Zhou, Heng Zhang, Peng Zhou, Junjie You, Gang Yao, Zhicheng Pan, Yang Liu, Bo Lai, 2022. *Heterogeneous photocatalyst-driven persulfate activation process under visible light irradiation: From basic catalyst design principles to novel enhancement strategies*. Chemical Engineering Journal,Volume 428, 131166.

[7]. Chengdu Qi, Xitao Liu, Jun Ma, Chunye Lin, Xiaowan Li, Huijuan Zhang, 2016. *Activation of peroxymonosulfate by base: Implications for the degradation of organic pollutants*. Chemosphere, Volume 151, Pages 280-288

[8]. Deepthi John, Jiya Jose, Sarita G. Bhat, V. Sivanandan Achari,2021. *Integration of heterogeneous photocatalysis and persulfate based oxidation using TiO_2-reduced graphene oxide for water decontamination and disinfection. Heliyon, 7, 7 e07451*

[9]. Mina Sabri, Aziz Habibi-Yangjeh, Srabanti Ghosh, 2020. *Novel $CuBi_2O_4$ heterostructures for persulfate-assisted photocatalytic degradation of dye contaminants under visible light*. Journal of Photochemistry and Photobiology A: Chemistry, Volume 391, 15, 112397.

[10]. Xiaoguang Duana, Hongqi Sunb, Moses Tadea, Shaobin Wanga, 2018. *Metal-free activation of persulfate by cubic mesoporous carbons for catalytic oxidation via radical and nonradical processes*. Catalysis Today Volume 307, Pages 140-146

[11]. Xinyu Du, Xue Bai, Lu Xu, Lei Yang, Pengkang Jin, 2019. *Visible-light Activation of Persulfate by TiO_2/g-C_3N_4 Photocatalyst toward Efficient Degradation of Micropollutants*. Chemical Engineering Journal, doi: https://doi.org/10.1016/j.cej.2019.12324

[12]. Luis M. Anaya-Esparza, Efigenia Montalvo-González, Napoleón González-Silva, María D. Méndez-Robles, Rafael Romero-Toledo, Elhadi M. Yahia, Alejandro Pérez-Larios, 2019. *Synthesis and Characterization of TiO_2-ZnO-MgO Mixed Oxide and Their Antibacterial Activity*. Materials, 12, 698.

[13]. Nguyen Dinh Tuyen, et al., 2022. *Synthesis of ternary metal oxides composites hybrid ZnO-MgO-TiO_2-polyphenol using orange leaf extracts for solar photocatalytic treament of bacteral/fungial diseases pathogens in agruculture cultivation.* Journal of Science & Technology, Chemistry Topic, p. 41-50

[14]. Elham Fakoori, Hassan Karami, Azizollah Nezhadali, 2019. *Synthesis and characterization of binary and ternary nanocomposites based on TiO_2, SiO_2 and ZnO*

with PVA based template-free gel combustion method. Materials Science-Poland, 37(3), pp. 426-436.

[15]. Máté Náfrádi, Tünde Alapi, Bence Veres, Luca Farkas, Gábor Bencsik, Csaba Janáky, 2023. *Comparison of TiO_2 and ZnO for Heterogeneous Photocatalytic Activation of the Peroxydisulfate Ion in Trimethoprim Degradation*. Materials, 16(17), 5920.

[16]. Da Oh, Zhili Dong, Teik-Thye Lim, 2016. *Generation of sulfate radical through heterogeneous catalysis for organic contaminants removal: Current development, challenges and prospects*. Applied catalysis B: EnvironmentalcVolume 194, Pages 169-201

[17]. A. Khan, M.M. Haque, Niyaz A. Mir, M. Muneer, C. Boxall, 2010. *Heterogeneous photocatalysed degradation of an insecticide derivative acetamiprid in aqueous suspensions of semiconductor*. Desalination 261, 169-174.

[18]. Jingzhe Xue, Zhihui Luo, Ping Li, Yaping Ding, Yi Cui, Qingsheng Wu, 2014. *A residue-free green synergistic antifungal nanotechnology for pesticide thiram by ZnO nanoparticles*. Scientific reports, 4, 5408 | DOI: 10.1038/srep05408

[19]. Hongqinv Huanga, Xiaochen Zhanga, 2016. *Integrated nanotechnology for synergism and degradation of fungicide SOPP using micro/nano- Ag_3PO_4*. Inorganic Chemistry Frontiers.

[20]. Ha Phuong Long, Nguyen Thi Nhan, Nguyen Thi Thu An, Cao Dinh Thanh, Nguyen Huy Cuong, Nguyen Duc Hai, Vu Minh Tan, Tran Duc Dai, Nguyen Thi Tuyet, Tran Thi My Duyen, Hoang Tung Duong, Nguyen Dinh Tuyen, 2020. *Preparation of solar photocatalyst based on multi oxides containing CeO_2/La_2O_3 from Vietnam rare earth ores and their antibacterial activeties for vibrio parahaemolyticus, staphylococcus aureus in aquatic/agriculture enviroment*. Journal of Science & Technology, Hanoi University of Industry, Vol. 56, No. 6, p.123.

THÔNG TIN TÁC GIẢ

Nguyễn Đình Tuyến[1], Nguyễn Thị Thu An[2], Nguyễn Quyết Tiến[1], Nguyễn Quảng An[1], Nguyễn Ngọc Trường[3], Nguyễn Thị Thục Anh[3], Nguyễn Huy Cường[3], Lê Thị Trang[3], Nguyễn Thị Mai[4]

[1]Viện Hóa Học, Viện Hàn lâm Khoa học và Công nghệ Việt Nam

[2]Viện Công nghệ Sinh học Viện Hàn lâm Khoa học và Công nghệ Việt Nam

[3]Viện Nghiên cứu Địa chất và Khoáng sản ứng dụng

[4]Trung tâm Phát triển Công nghệ cao, Viện Hàn lâm Khoa học và Công nghệ Việt Nam